J. Min. Metall. Sect. B-Metall. 51 (2) B (2015) 143 - 151

Journal of Mining and Metallurgy, Section B: Metallurgy

PROPERTIES AND APPLICATION OF CARBON COMPOSITE BRICK FOR BLAST FURNACE HEARTH

K.X. Jiao[a,b], J.L. Zhang[a,b], Z.J. Liu[a,b], Y.G. Zhao[c], X.M. Hou[a,b,*]

[a] School of Metallurgical and Ecological Engineering, University of Science and Technology Beijing, Beijing, China
[b] State Key Laboratory of Advanced Metallurgy, University of Science and Technology Beijing, Beijing, China
[c] Henan Winna Industrial group Co. Ltd, Gongyi, Henan, China

(Received 07 November 2014; accepted 06 April 2015)

Abstract

A type of carbon composite brick was produced via the microporous technique using natural flack graphite, α-Al_2O_3 and high-quality bauxite chamotte (Al_2O_3≥87 mass%) as raw materials with fine silicon powder as additive. The composition and microstructure of the obtained carbon composite were characterized using chemical analysis, XRD and SEM with EDS. The high temperature properties of thermal conductivity, oxidization and corrosion by molten slag and hot metal of the composite were analyzed. Based on these, the type of carbon composite brick worked in a blast furnace hearth for six years was further sampled at different positions. The protective layer was found and its chemical composition and microscopic morphology were investigated. It is found that the carbon composite brick combines the good properties of both the conventional carbon block and ceramic cup refractory. The protective layer near the hot face consists of two separated sublayers, i.e. the slag layer and the carbon layer. A certain amount of slag phase is contained in the carbon layer, which is caused by the reaction of coke ash with the refractory. No obvious change in the chemical composition of the protective layer along the depth of the sidewall is found. This work provides a useful guidance for the extension of the lifetime of blast furnace hearths.

Key words: blast furnace; hearth; carbon composite brick; the protective layer

1. Introduction

To ensure the safe and smooth operation of the blast furnace and to extend its service life are two main technological trend of the modern large blast furnace. Hearth is an important component of blast furnace. The safety condition of the hearth determines the blast furnace campaign to large degree [1-2]. At present, in some plants, the breakout of blast furnace hearths takes place very often. The main reason is attributed to the severe infiltration of hot metal into the refractory lining. Therefore the key factor to expand the lifespan of the hearth is to improve the refractory quality [3]. Traditionally, the hearth refractory lining structure mainly consists of carbon blocks and ceramic cup [4-5]. However, both these two kinds of material have instinct disadvantages. For example, the corrosion resistance of conventional carbon blocks to hot metal is very poor. In addition, the low thermal conductivity of ceramic cup tends to cause extremely high hot face temperature which is unfavorable to the formation of protective layer. These disadvantages directly cause the damage of hearth structure and thus reduce the blast furnace campaign life [6-8].

To prevent penetration of molten iron, some measures have been taken. For instance, it is an effective way to reduce the pore size of the carbon block into micro-pores by formation of Si-O-N whiskers within the pores. In addition, alumina is added in the block to reduce the interacting surface area of carbon with molten iron. The reason is that alumina possesses excellent high temperature strength and good resistance to mechanical wear [9-10]. Therefore Al_2O_3-C refractory has been widely used in the continuous casting process of iron & steel industry due to its excellent mechanical properties, thermal shock resistance and corrosion resistance [11-13]. However the traditional Al_2O_3-C refractory is rarely adopted in blast furnace hearth due to its low coefficient of thermal conductivity. Thus refractory with high coefficient of thermal conductivity needs to be developed. Recently a new type of carbon composite brick has been developed by mixing the carbon composition with a proper amount of oxide and silicon fine powder using the resin as binder. The obtained carbon composite brick combines the advantages of both the conventional carbon block and the ceramic cup. This type of carbon composite brick has been successfully applied in an iron & steel plant

* *Corresponding author: houxinmei01@126.com*

DOI:10.2298/JMMB141107018J

and worked for six years without relining. In addition, the monitoring system such as thermocouples also reveals the steady and low temperature along the sidewall and no obvious sign of corrosion [14-15].

In this paper, the properties of this type of carbon composite brick such as the thermal conductivity and corrosion resistance etc. were analyzed. Furthermore the protective layer was sampled when the blast furnace was blown down for a regular maintenance. By carrying out these investigations, the long-lifespan mechanism of the blast furnace hearth using carbon composite brick is explored.

2. Experimental

2.1. Preparation of the carbon composite brick

Natural flack graphite, α-Al_2O_3 and high-quality bauxite chamotte (Al_2O_3, ≥87 mass%) with a certain ratio used as raw materials were mixed, ground and pressed into bricks. In addition, a certain amount of fine silicon powder was used as additive. The bricks were dried and fired at 1650 °C for 10 h at a reducing atmosphere. The phase compositions of the fired specimens were analyzed by X-ray diffraction (Shimadzu XRD-1800, Japan). The microstructures of ruptured surfaces of carbon composite brick were observed by a field emission scanning electron microscope equipped with an energy dispersive X-ray spectroscope (JEOL JSM-5600LV, Japan).

2.2 *Properties of the carbon composite brick*

The laser method was employed to measure the thermal diffusivity of the carbon composite brick with 10mm in diameter and 5-10mm in thickness. The thermal conductivity was calculated based on the one dimensional transient heat flow equation as following:

$K=\alpha\cdot\rho\cdot C_p$.

Where α, ρ, C_p are the diffusivity (m^2/s), density (g/cm^3) and specific heat (J/(g·K)) of the sample respectively.

As for the oxidation experiment, it was carried out on a non-isothermal mode. The sample with 50mm in diameter and 50mm in height was heated from room temperature to 1400 °C at a certain heating rate in flowing air.

In view of the iron and slag erosion experiment, the sample was made into a crucible with 50mm in outer diameter and 25mm in inner diameter. In the experiment, the iron and slag taken from the iron and steel enterprise were put into the crucible respectively and heated up to 1500 °C for 2 h in argon atmosphere. The chemical composition of blast furnace slag and hot metal used in this experiment were showed in Table 1 and 2.

Table 1. *Chemical composition of molten slag*

Chemical composition	SiO_2	CaO	MgO	Al_2O_3	R
Content, wt%	31.92	36.36	9.89	15.11	1.14

Table 2. *Chemical composition of hot metal*

Chemical composition	C	Si	Mn	P	S
Content, wt%	4.76	0.46	0.33	0.059	0.029

2.3 Characterization of the sample after practical application

After the carbon composite brick was applied in an iron & steel plant for six years, the blast furnace was blown down with iron remained in the hearth in order to carry out a shotcrete lining for stack. The water temperature during operation was measured and the remaining thickness of the block was estimated. The location was selected from No.1tuyere besides the taphole where the remaining thickness of the block was estimated to be minimum in the circumferential direction. During the remaining clean-up process, the samples of the protective layer located at different height of the location were taken for analysis. Sampling positions were showed in Figure 1. All the sampling locations were below No.1 tuyere and away from the centerline of the blowpipe at a downward distance of 2.1 m, 2.25 m, 2.6 m and 2.8 m respectively. Samples obtained from the four sections in different height were marked as (a), (b), (c) and (d). It should be noted that the vertical distance between the centerline of the blowpipe and of the taphole was 2.25 m. Meanwhile, the microstructure of samples was damaged as little as possible. A variety of techniques such as chemical analysis, scanning electron microscope (SEM), X-ray diffraction (XRD) were introduced to examine the adhesion protective layer.

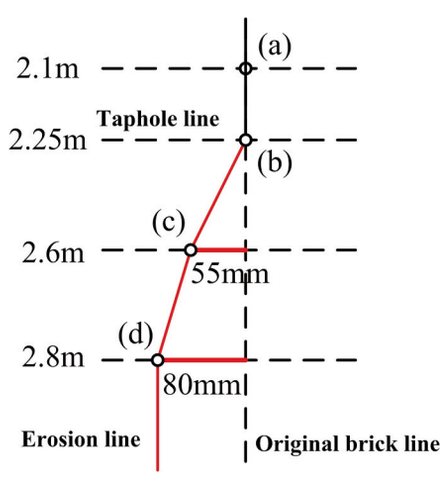

Figure 1. *Samples obtained from different height under No.1 tuyere*

3. Results and discussions

3.1 The chemical component of the carbon composite brick

The chemical component of the carbon composite bricks is showed in Table 3. From the table, the main chemical components in the carbon composite brick are Al_2O_3 and C. A certain amount of SiO_2 and SiC are contained in the brick. Other impurities such as TiO_2 and Fe_2O_3 etc. with low content are also exist. The impurities mainly come from bauxite.

Table 3. *The chemical component of the carbon composite bricks*

chemical component	Al_2O_3	C	SiO_2	TiO_2	Fe_2O_3	Na_2O	K_2O	SiC
content, wt%	73.05	10.2	8.18	1.2	0.9	0.29	0.11	6

3.2 Phase and microstructure of the carbon composite brick

Figure 2 shows the XRD pattern of the obtained carbon composite brick. It can be seen that the major crystalline phases are Al_2O_3 and C. The phase of $3Al_2O_3{\cdot}2SiO_2$ appears via the reaction of Al_2O_3 with SiO_2 at elevated temperature. SiC is also detected which is caused by the reaction of silicon with carbon.

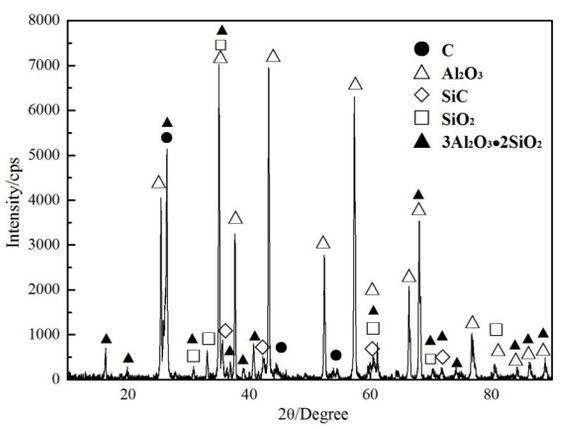

Figure 2. *XRD pattern of the synthesized carbon composite brick*

The microstructure of the carbon composite brick is shown in Figure 3. It reveals the brick possesses a porous microstructure. The average size of the pores analysized by AutoPore IV 9500(USA) [16] is to be 0.238μm. The pores are uniformly distributed in the matrix (Figure 3a). Inside the pores, large amount of fibers exist as shown in Figure 3b. EDS analysis indicates that the fibers are SiC.

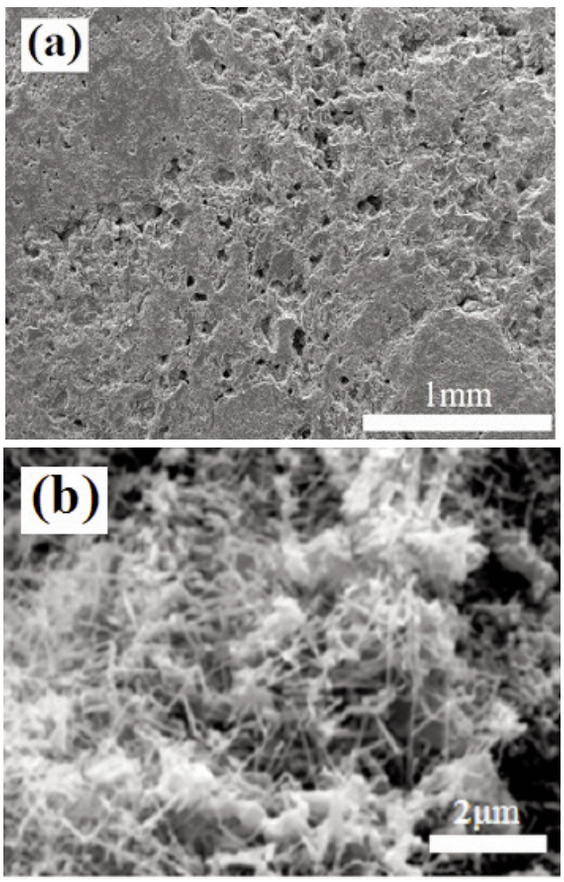

Figure 3. *Microstructure of the carbon composite brick*

3.3 Properties of the carbon composite brick

The properties of the carbon composite brick are listed in Table 4. For comparison, the properties of several kinds of common refractory are also listed in Table 4 [17-19]. It is well known that the main advantage of the conventional carbon brick is the high thermal conductivity. But its shortcomings are the low corrosion resistance to both molten slag and hot metal and poor resistance to oxidation. As for the ceramic cup, the corrosion resistance to molten slag is poor.

By comparison, the corrosion resistance index of the new type of the carbon composite brick is 0.62%, which is comparable to that of the traditional ceramic cup. Moreover, it exhibits excellent oxidation resistance. The main reason is that the promoting sintering process results in a dense microstructure. Meanwhile SiC formed in the carbon composite brick also reduces the porosity (as shown in Figure 3b). In addition, crystalline phase such as $3Al_2O_3{\cdot}2SiO_2$ formed within the carbon composite brick leads to a volume expansion, which is also responsible for decreasing the porosity of the brick.

Table 4. *Properties of different types of refractory materials*

Properties		Carbon composite brick	Brown fused alumina	Corundum-mullite brick	NMA	Conventional Carbon block
Pxdization rate, %		0.9	0	0	18.06	8.89
Corrosion resistance index to hot metal, %		0.62	0	0.54	28.18	25.65
Corrosion resistance index to slag, %		1.81	23.08	57	--	--
Thermal conductivity, W/(m·K)	30℃	17.34	6.35	4.16	4.96	6.55
	300℃	16.21	4.93	4.48	11.3	11.55
	600℃	14.27	5.42	4.46	16.1	13.38
	800℃	13.78	4.61	5.08	16.6	13.55

3.3.1 Coefficient of thermal conductivity

From Table 4, it can be seen that the thermal conductivity of the carbon composite brick is up to 13 W/(m·K), which is capable of meeting the requirement of the blast furnace hearth. The temperature dependence of thermal conductivity of the carbon composite brick is shown in Figure 4.

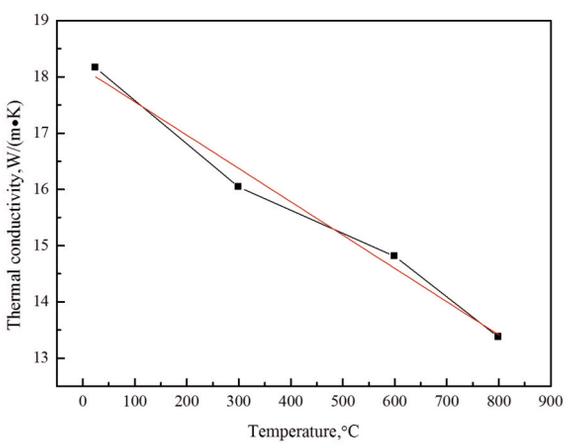

Figure 4. *Temperature dependence of thermal conductivity of the carbon composite brick*

The mathematical relation between temperature and thermal conductivity could be obtained by least squares linear regression as follows.

$\lambda = -0.00529T + 18.149$

Where λ and T represent the thermal conductivity(W/(m·°C)) and the temperature of carbon composite brick(°C).

The linear correlation coefficient, R^2 is 0.9777. From Figure 4, it can be seen that the average thermal conductivity of the carbon brick is higher than the conventional carbon brick. The main reason is the formation of the dense network structure due to the interaction between silicon and carbon which is conducive to the heat transfer.

The thermal conductivity of the carbon composite brick in the work decreases with temperature increasing. According to the microscopic mechanism of thermal conductivity [20-23], the conducting of heat within inorganic materials is the result of the phonon collision. The thermal conductivity coefficient mainly depends on the degree of deviation of lattice vibration resonance. Therefore the reason of the carbon composite brick decreasing with temperature is attributed to the deficiency in the amount of free electrons and thus has a poor ability of conducting heat.

3.3.2 Corrosion resistance to the molten slag

Figure 5 is the experimental result of SEM with EDS of the carbon composite brick after the molten slag corrosion. It can be seen that the molten slag contacts with the carbon composite brick well, indicating good wettability between them. The occurrence of a large quantity of slag components in the interior of the carbon composite brick (shown in EDS analysis of area B of Figure 5) reveals that the molten slag gradually penetrates into the carbon composite brick. The newly formed pores due to the corrosion promote the diffusion process and finally destroy the structure of the carbon composite brick [24-26].

However, the damage caused by the corrosion of the molten slag barely occurs in practical application. The main reason is that the increasing content of Al_2O_3 in the molten slag resulting from the reaction between the molten slag and the carbon composite brick significantly increases the viscosity of the molten slag. At the same time, the cooling effect in the bottom and hearth of the blast furnace promotes the precipitation of magnesium aluminate spinel, which could also increase the viscosity of the molten slag. Therefore the molten slag is difficult to infiltrate into the interior of the carbon composite brick.

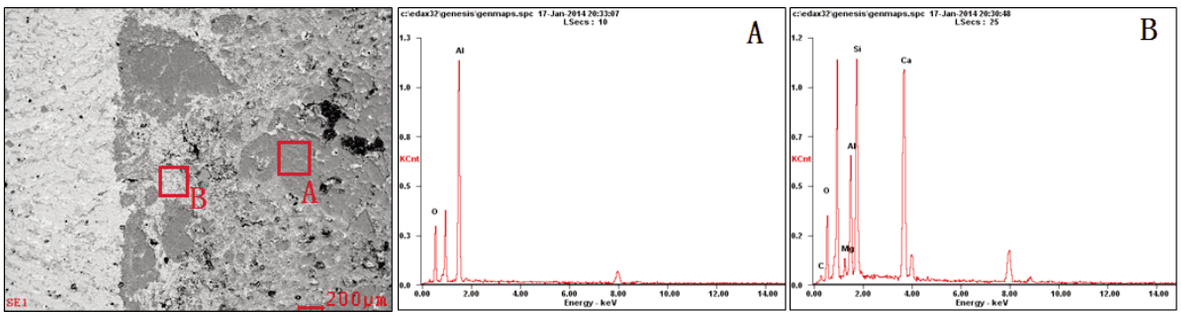

Figure 5. *SEM with EDS of the carbon composite brick after corrosion by molten slag*

3.3.3 Corrosion resistance to hot metal

Figure 6 shows SEM with EDS of the carbon composite brick after corrosion by hot metal. The carbon composite brick and hot metal can be separated easily after experiment. On the contact surface (area B) as shown in Figure 6, carbon is rich with tiny Al_2O_3 particles dispersed in the carbon matrix. The main reason is possible as follows. In the experiment, temperature decreasing causes the precipitated carbon from hot metal to enter into Al_2O_3 particles. Al_2O_3 particles tend to be broken into small particles due to internal stresses.

In practice, a temperature boundary layer is formed between the flowing hot metal and the carbon composite brick by adopting of the hearth bottom cooling system. The solubility of carbon in the boundary is decreased and the carbon in the hot metal is precipitated. In addition, the presence of the solid Al_2O_3 particles as well as the carbon particles increases the viscosity of hot metal and thus prevents these particles being washed away. Consequently, the carbon composite brick could not contact hot metal directly and thus the carbon composite brick is well protected.

3.4 Analysis of the protective layer

3.4.1 Chemical analysis and phase of the protective layer

Sample obtained from the four sections in different height were marked as (a), (b), (c) and (d) respectively. The photos of the samples shown in Figure 6 illustrate that these samples share a certain degree of similar features, i.e. the samples of the protective layer are divided into two layers obviously. The part near the hot face of the refractory lining has a black color and the thickness of the black part is small. In addition, the part adjacent to the black part is very hard and the color is light gray.

Sample (c) is taken for analysis. The two layers can be separated manually. The black layer is mainly consisted of carbon and the gray layer is slag. The chemical composition of the slag layer as well as of blast furnace slag is compared in Table 5. Obviously the composition of the slag layer is rich in Al_2O_3, which is different from that of blast furnace slag. Therefore it can be confirmed that the source of the protective layer is not derived from blast furnace slag.

Table 5. *Chemical composition of the slag layer and blast furnace slag*

Composition, %	CaO	SiO_2	Al_2O_3	MgO	Fe	R
The slag layer	38.74	22.96	22.83	10.18	5.3	1.69
Blast furnace slag	36.36	31.92	15.11	9.89	-	1.14

Figure 8 shows the XRD patterns of the four protective layer samples. Figure 8 (a) is corresponding to Sample (a). It shows that the main crystalline phases are carbon, $Al_2O_3{\cdot}SiO_2$, $3Al_2O_3{\cdot}2SiO_2$, $Ca_2AlSi_2O_7$, $MgAl_2O_4$ and Fe. Figure 8 (b), (c) and (d) are the slag layer of sample (b), (c) and (d) respectively. It can be seen that the phase

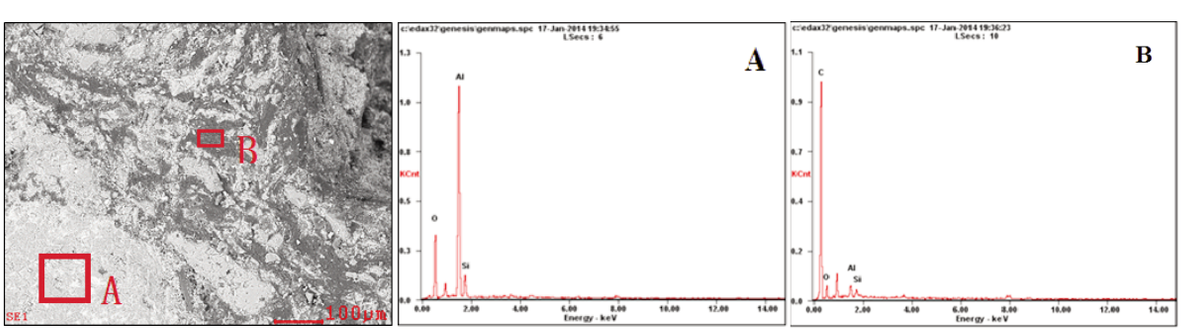

Figure 6. *SEM with EDS of the carbon composite brick after corroded by hot metal*

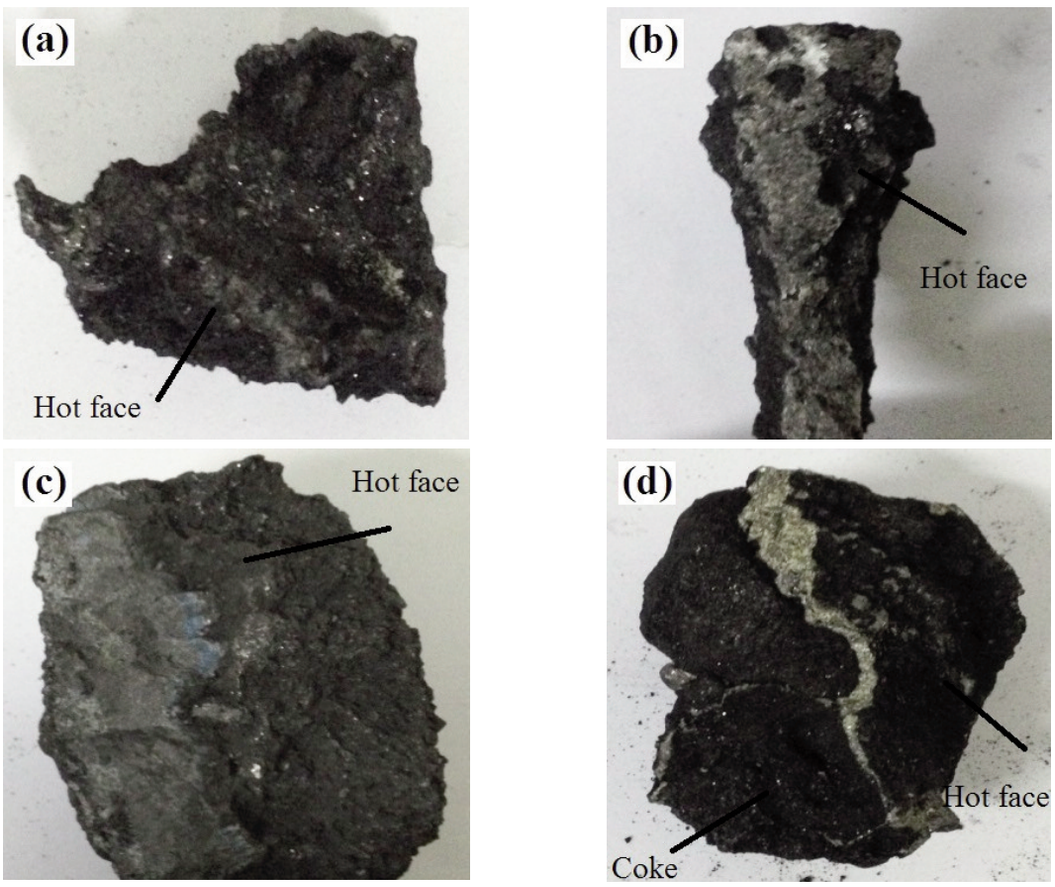

Figure 7. *Photos of the samples obtained at different height: (a) 2.1m; (b) 2.25m; (c) 2.6m; (d) 2.8m.*

composition of the three samples are similar, i.e. $Al_2O_3 \cdot SiO_2$, $3Al_2O_3 \cdot 2SiO_2$, $Ca_2AlSi_2O_7$ and $MgAl_2O_4$. Therefore, the phase composition of the protective layer is not changed markedly along the depth of the blast furnace hearth direction.

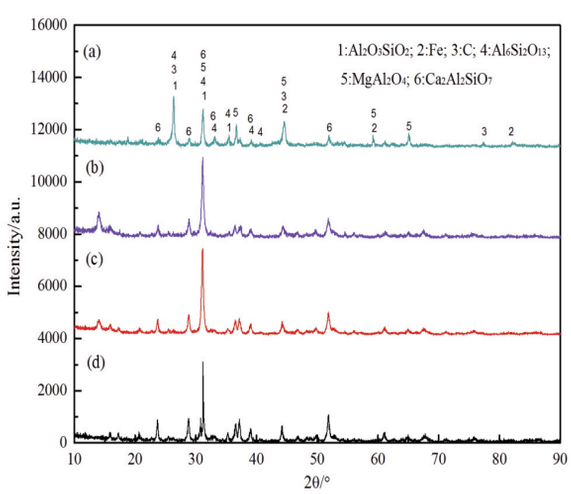

Figure 8. *XRD patterns of the four protective layers obtained at different height: (a) 2.1m; (b) 2.25m; (c) 2.6m; (d) 2.8m*

3.4.2 Microstructure of the protective layer

Figure 9 is SEM with EDS of the protective layer. Obviously, layered character of the protective layer is observed. For sample A, carbon is the main component in area 1 while Al_2O_3 is rich in area 2. Based on the microstructure of the refractory materials used in this blast furnace hearth, it could be determined that the left part with major component of carbon and Al_2O_3 is the carbon composite brick while the right side whose major component is carbon is the protective layer closely attached to the surface of the refractory lining. Moreover EDS analysis reveals that a tiny amount of potassium is penetrated into the carbon composite brick. For sample (b), (c) and (d), the appearance of interface next to the carbon composite brick are consisted of two layers. The left side is adjacent to the carbon composite brick and the right side is adjacent to the hot metal. The protective layer on the right is mainly slag phase while the chemical composition does not change much. By contrast, the left side is rich in carbon mixed with the slag phase with different sizes and shapes.

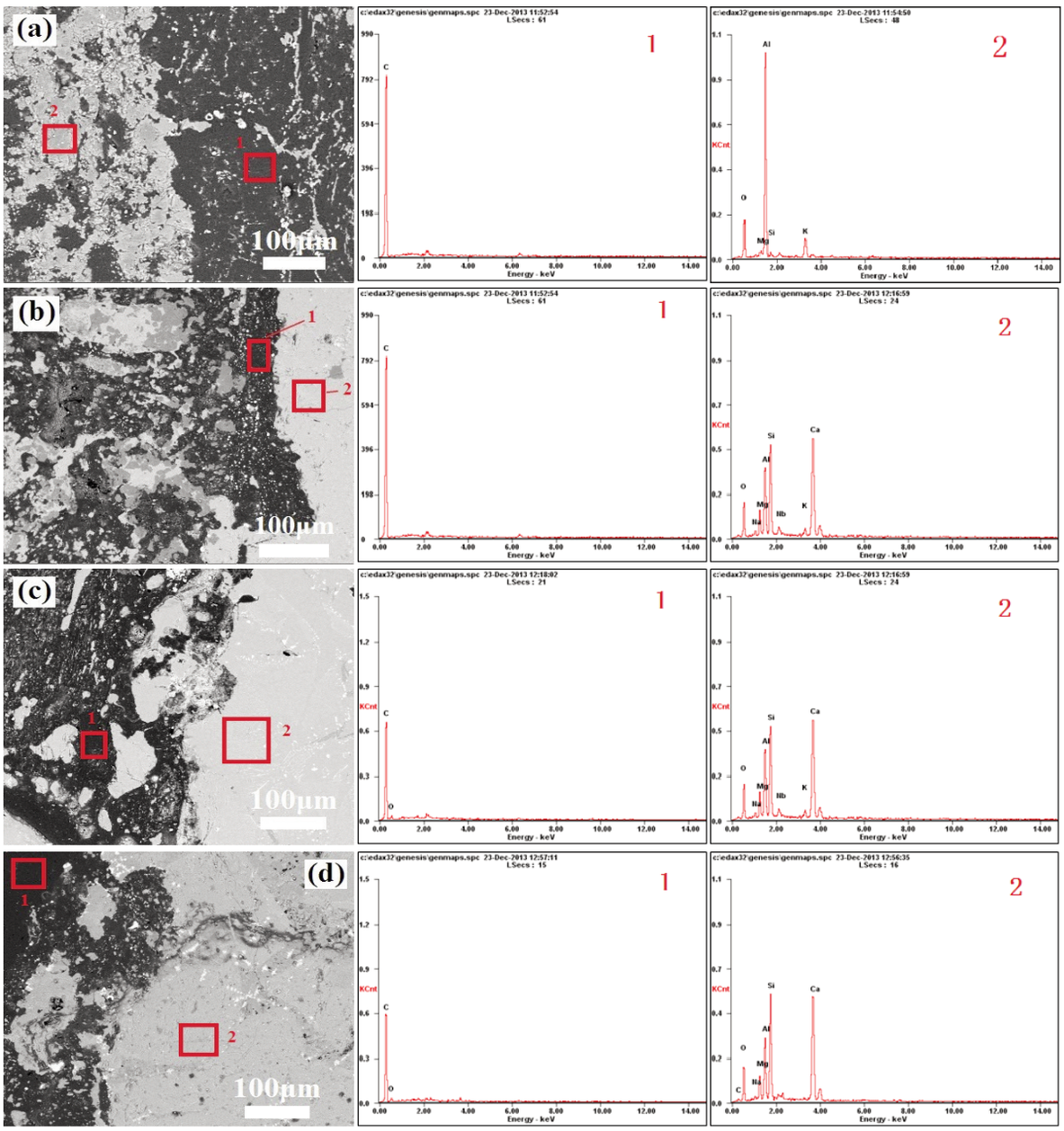

Figure 9. *SEM with EDS analysis of the protective layer: (a) 2.1m; (b) 2.25m; (c) 2.6m; (d) 2.8m*

3.4.3 The formation mechanism of the protective layer

From above experimental results, the formation mechanism of the protective layer is discussed in this section. In view of the formation of slag layer, the blast furnace hearth is filled with coke in the normal production. Because the density of the slag is smaller than hot metal, it tends to float on the top of hot metal. As a result, only hot metal and coke exist below the centerline of the taphole [27-29]. Therefore it is easy for the refractory lining to contact with coke as shown in Figure 7 (d). The interaction between hot metal and coke lead the carburization reaction to occur. Therefore the coke ash is left and further reacts with Al_2O_3 to form slag phase. Since the viscosity of slag phase is higher than that of hot metal, the velocity of hot metal is slowed down and the convective heat transfer is reduced when it flows around the viscous layer. In addition, the low coefficient of hot metal further reduces the hot face temperature of the carbon composite brick lining. As a result, a layer of slag is formed.

When the cooling intensity to the hot face of the block is weak, a protective layer is not formed in a stable manner. When the cooling to the hot face is strong or the temperature changes in the furnace, the solubility of carbon in molten iron is reduced. Carbon from the hot metal in the furnace diffuses toward proeutectic graphite and precipitates, which results in the carbon thickness increasing. As a result, proeutectic graphite grows and a layer of high carbon concentration is formed.

For the chemical composition of the slag in the protective layer, MgO accounts for 10.18 wt%. With the content of MgO being fixed, the quaternary phase diagram of CaO-MgO-SiO_2-Al_2O_3 system can be calculated via Factsage software as shown in Figure 10. With the temperature lowing, Al_2O_3 tends to combine with MgO partially to form high melting point phase, i.e. $MgAl_2O_4$.

In practice $MgAl_2O_4$ in the slag is precipitated as solid particles on the hot face of the refractory as shown in Figure 11. This increases the viscosity of the viscous layer and thus is capable of protecting the refractory lining effectively. When the thickness of the viscous layer is increased to a certain level, the temperature of the viscous layer increases and carbon in hot metal is unable to precipitate. As a result, the protective layer formed in later stage rarely contains carbon, indicating the thickness of the viscous layer reaches a stable value. Due to the formation of a protective layer of high carbon concentration and slag, it prevents the dissolution of carbon of the block as a buffer between hot metal and the block.

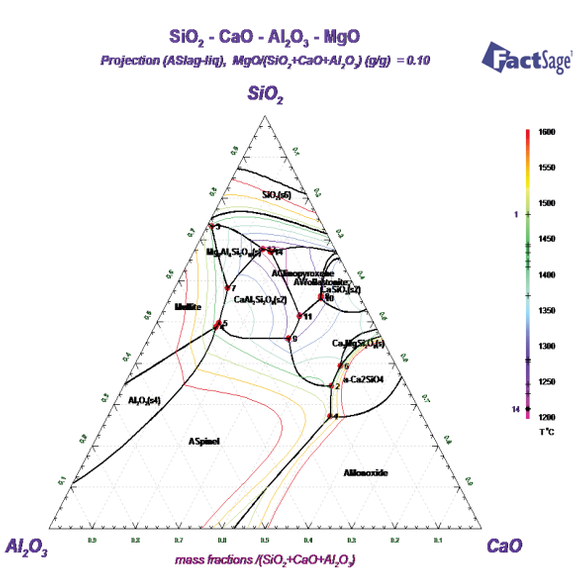

Figure 10. *Ternary phase diagram of CaO -SiO_2-Al_2O_3 system.*

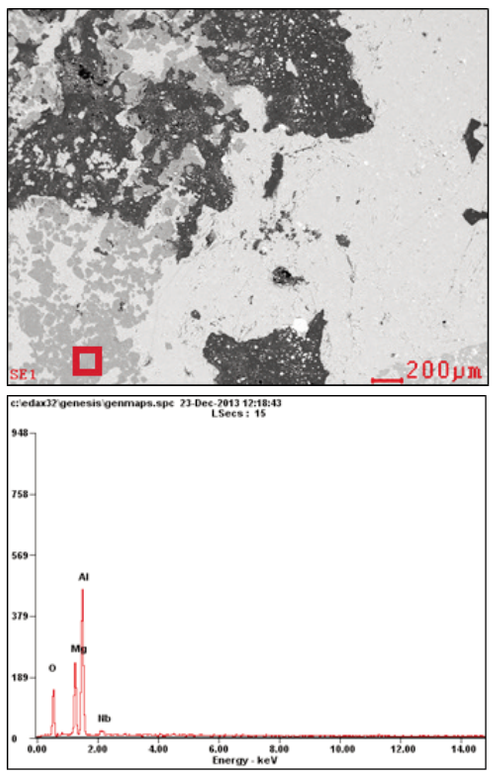

Figure 11. *SEM image and EDS spectra of the precipitated $MgAl_2O_4$*

4. Conclusions

A type of carbon composite brick was produced via the microporous technique. The high temperature properties of thermal conductivity, oxidization and corrosion by molten slag and hot metal of the composite were analyzed. The results show that the obtained carbon composite brick combines the good properties of both the conventional carbon block and ceramic cup refractory due to its dense network structure. During the practical application, this type of carbon composite brick used as blast furnace hearths also exhibits excellent performance. The protective layer is found in hearth. It consists of two layers. One is carbon layer. The other is slag layer. The source of the slag phase is the product of the interaction between coke ash in deadman and the refractory lining. The carbon layer is derived from the graphite precipitation from hot metal at low temperature.

Acknowledgements

The authors express their appreciation to NSFC(Natural Science Foundation of China) (No. 51304014), Natural Science Foundation of China and Baosteel under Grant (No. 51134008) and Program for Changjiang Scholars and Innovative Research Team in University (IRT1207) for financial support.

Reference

[1] S.J. Nam, J. Sang, Y.B. Kang, ISIJ Int., 53(2013) 1779.

[2] Z.J. Liu, J.L. Zhang, T.J. Yang, Asia Steel 2012, September 24-26, Beijing, China, 2012, p.1123.

[3] F.M. Zhang, J. Iron Steel Res. Int., 20 (2013) 53.

[4] Y. Zhang, D. Rohit, D. Frank, Int. J. Heat Mass & Transfer, 51(2008) 186.

[5] Z.J. Liu, J.L. Zhang, T.J. Yang, ISIJ Int., 52 (2012) 1713.

[6] L.J. Wu, W.G. Zhou, H.E. Cheng, Int. J. Adv. Manuf. Tech., 29(2006) 64.

[7] H.B. Zhao, S.F. Hu, S.S. Cheng, Int. J. Min. Met. Mater., 20(2013) 345.

[8] H. Wang, Y. Li , T. Zhu, Ceram. Int., 40(2014) 11139.

[9] L.A. Díaz, R. Torrecillas, J. Eur. Ceram. Soc., 27(2007) 4623.

[10] Y. Li, Y. Li, S. Sang, Metall. Mater. Trans. A, 45(2014) 477.

[11] M. Luo, Y.W.Li, S.L.Jin, Mater. Sci. Eng. A, 548(2012) 134.

[12] Q. Zhu, W.J.Zhang, Y.S.Yao, Refract., 40(1) (2006) 90.

[13] B.Q. Zhu, Y.N.Zhu, X.C.Li, Ceram. Int., 39 (2013) 6069.

[14] C.H. Lin, W.T. Cheng, S.W. Du. Int. Commun. Heat & Mass, 36(2009) 335.

[15] B. Johnny, S. Henrik, Chem. Eng. Sci., 59(2004) 3423.

[16] Z.H. Tian, X.H. Zhang, M.H. Mei., PTCA, 49(2013) 615.

[17] M.S. Song, Z.J. Yu. Ironmak. & Steelmak., 27(2008) 1.

[18] R.T. Xu, R.S. He, Y.G. Cao, 2012 national meeting of high blast temperature and longevity of BF, April 26-28, Beijing, China, 2012, p. 234.

[19] S.R. Zhang, J. Iron Steel Res. Int., 13(2006) 1.

[20] S.R. Zhang, Z.J. Yu, The blast furnace abnormal and accident treatment, Metallurgical Industry Press, Beijing, 2012, p.111.

[21] T. Ebadzadeh, M. Heidarzadeh-Tari, C. Falamaki, Adv. Appl. Ceram, 108 (2009) 369.

[22] A.S. Muhammad, S. Hidekazu, J. Eur. Ceram. Soc, 28 (2008) 311.

[23] M.N. Khezrabadi, J. Javadpour, H.R. Rezaie, R. Naghizadeh, J. Mater. Sci, 41 (2006) 3027.

[24] L.H. Zou, B.Y. Huang, Q.Z. Huang, T. Nonferr. Metal soc., 7(1997) 132.

[25] J.Y. Zhang, Physical chemistry in metallurgy, Metallurgical Industry Press, Beijing, 2007, p.305.

[26] D. Yang, Y. Liu, M. Fang, Ceram. Int., 40(2014) 1593.

[27] L.A. Díaz, R. Torrecillas, A.H. deaza, J. Eur. Ceram. Soc., 27(2007) 4623.

[28] J.L. Zhang, G.S. Wang, Energy, 33(2008) 525.

[29] T. Inada, A. Kasai, K. Nakano, ISIJ Int., 49(2009) 470.